ELSEVIER

28 December 2000

PHYSICS LETTERS B

Physics Letters B 496 (2000) 137–144

www.elsevier.nl/locate/npe

Observation of the decay $K_S \to \pi^+\pi^-e^+e^-$

A. Lai, D. Marras, L. Musa

Dipartimento di Fisica dell'Università e Sezione dell'INFN di Cagliari, I-09100 Cagliari, Italy

A. Bevan, R.S. Dosanjh, T.J. Gershon, B. Hay [7], G.E. Kalmus, D.J. Munday, M.D. Needham [1], E. Olaiya, M.A. Parker, T.O. White, S.A. Wotton

Cavendish Laboratory, University of Cambridge, Cambridge, CB3 0HE, UK [2]

G. Barr, H. Blümer, G. Bocquet, A. Ceccucci, D. Cundy, G. D'Agostini, N. Doble, V. Falaleev, L. Gatignon, A. Gonidec, G. Govi, P. Grafström, W. Kubischta, A. Lacourt, A. Norton, S. Palestini, B. Panzer-Steindel, B. Peyaud [3], H. Taureg, M. Velasco, H. Wahl

CERN, CH-1211 Genève 23, Switzerland

C. Cheshkov, P. Hristov [7], V. Kekelidze, D. Madigojine, A. Mestvirishvili [4], N. Molokanova, Yu. Potrebenikov, G. Tatishvili [7], A. Tkatchev, A. Zinchenko

Joint Institute for Nuclear Research, Dubna, Russian Federation

I. Knowles, V. Martin [5], H. Parsons, R. Sacco, C. Lazzeroni [6], A. Walker

Department of Physics and Astronomy, University of Edinburgh, JCMB King's Buildings, Mayfield Road, Edinburgh, EH9 3JZ, UK

M. Contalbrigo, P. Dalpiaz, J. Duclos, P.L. Frabetti, A. Gianoli, M. Martini, F. Petrucci, M. Savrié

Dipartimento di Fisica dell'Università e Sezione dell'INFN di Ferrara, I-44100 Ferrara, Italy

A. Bizzeti [8], M. Calvetti, G. Collazuol, G. Graziani, E. Iacopini, M. Lenti [7]

Dipartimento di Fisica dell'Università e Sezione dell'INFN di Firenze, I-50125 Firenze, Italy

H.G. Becker, M. Eppard, H. Fox, K. Holtz, A. Kalter, K. Kleinknecht, U. Koch, L. Köpke, I. Pellmann, A. Peters, B. Renk, S.A. Schmidt, V. Schönharting, Y. Schué, A. Winhart, M. Wittgen

Institut für Physik, Universität Mainz, D-55099 Mainz, Germany [9]

J.C. Chollet, S. Crépé, L. Fayard, L. Iconomidou-Fayard, J. Ocariz, G. Unal, I. Wingerter-Seez

Laboratoire de l'Accélérateur Linéaire, IN2P3-CNRS,Université de Paris-Sud, 91406 Orsay, France [10]

0370-2693/00/$ – see front matter
PII: S0370-2693(00)01300-9

G. Anzivino, P. Cenci, E. Imbergamo, P. Lubrano, A. Nappi, M. Pepe, M. Piccini

Dipartimento di Fisica dell'Università e Sezione dell'INFN di Perugia, I-06100 Perugia, Italy

R. Carosi, R. Casali, C. Cerri, M. Cirilli, F. Costantini, R. Fantechi, S. Giudici, B. Gorini, I. Mannelli, G. Pierazzini, M. Sozzi

Dipartimento di Fisica dell'Università, Scuola Normale Superiore e Sezione dell'INFN di Pisa, I-56100 Pisa, Italy

J.B. Cheze, J. Cogan, M. De Beer, P. Debu, A. Formica, R. Granier de Cassagnac, E. Mazzucato *, R. Turlay, B. Vallage

DSM/DAPNIA–CEA Saclay, F-91191 Gif-sur-Yvette cedex, France

I. Augustin, M. Bender, M. Holder, M. Ziolkowski

Fachbereich Physik, Universität Siegen, D-57068 Siegen, Germany [11]

R. Arcidiacono, C. Biino, F. Marchetto, E. Menichetti, N. Pastrone

Dipartimento di Fisica Sperimentale dell'Università e Sezione dell'INFN di Torino, I-10125 Torino, Italy

J. Nassalski, E. Rondio, M. Szleper, W. Wislicki, S. Wronka

Soltan Institute for Nuclear Studies, Laboratory for High Energy Physics, PL-00-681 Warsaw, Poland [12]

H. Dibon, G. Fischer, M. Jeitler, M. Markytan, I. Mikulec, G. Neuhofer, M. Pernicka, A. Taurok

Österreichische Akademie der Wissenschaften, Institut für Hochenergiephysik, A-1050 Wien, Austria [13]

Received 26 October 2000; accepted 15 November 2000
Editor: W.-D. Schlatter

* Corresponding author.
E-mail address: edoardo@hep.saclay.cea.fr (E. Mazzucato).

[1] Present address: NIKHEF, PO Box 41882, 1009 DB Amsterdam, The Netherlands.

[2] Funded by the UK Particle Physics and Astronomy Research Council.

[3] On leave from DSM/DAPNIA-CEA Saclay, F-91191 Gif-sur-Yvette cedex, France.

[4] Present address: Dipartimento di Fisica dell'Università e Sezione dell'INFN di Perugia, I-06100 Perugia, Italy.

[5] Present address: Department of Physics and Astronomy, Northwestern University, 2145 Sheridan Road, Evanston, IL 60208, USA.

[6] Present address: Cavendish Laboratory, University of Cambridge, CB3 0HE, UK.

[7] Present address: EP Division, CERN, 1211 Genève 23, Switzerland.

[8] Dipartimento di Fisica dell'Università di Modena e Reggio Emilia, via G. Campi 213/A I-41100, Modena, Italy.

[9] Funded by the German Federal Minister for Research and Technology (BMBF) under contract 7MZ18P(4)-TP2.

[10] Funded by Institut National de Physique des Particules et de Physique Nucléaire (IN2P3), France.

[11] Funded by the German Federal Minister for Research and Technology (BMBF) under contract 056SI74.

[12] Supported by the KBN under contract SPUB-M/CERN/P03/DZ210/2000 and using computing resources of the Interdisciplinary Center for Mathematical and Computational Modeling of the University of Warsaw.

[13] Funded by the Austrian Ministry for Traffic and Research under the contract GZ 616.360/2-IV GZ 616.363/2-VIII, and by the Fonds für Wissenschaft und Forschung FWF Nr. P08929-PHY.

Abstract

We present the first observation of the decay $K_S \to \pi^+\pi^-e^+e^-$ based upon the data collected in 1998 by the NA48 experiment at CERN. We have identified a clean sample of 56 events with negligible background contamination. Using $K_L \to \pi^+\pi^-\pi^0_D$ decays as normalization sample, the branching ratio is measured to be $BR(K_S \to \pi^+\pi^-e^+e^-) = [4.5 \pm 0.7(stat) \pm 0.4(syst)] \times 10^{-5}$. This result is in good agreement with the theoretical expectations from the mechanism of inner bremsstrahlung.

1. Introduction

The study of neutral kaon decays into the $\pi^+\pi^-e^+e^-$ final state has recently aroused considerable interest from both the theoretical and the experimental points of view. The $K_{L,S} \to \pi^+\pi^-e^+e^-$ decays are expected to proceed through a virtual photon intermediate state $K_{L,S} \to \pi^+\pi^-\gamma^* \to \pi^+\pi^-e^+e^-$ [1,2]. In the case of the long-lived neutral kaon, the amplitude for this decay is dominated by two components: one from the CP-conserving direct emission process (DE) associated with a magnetic dipole transition (M1), the other one from the CP-violating $K_L \to \pi^+\pi^-e^+e^-$ decay with inner bremsstrahlung (IB). The interference of the CP-even and CP-odd amplitudes produces a CP-violating circular polarization of the virtual photon which gives rise to a large asymmetry in the distribution of the angle Φ between the $\pi^+\pi^-$ and e^+e^- planes in the kaon centre of mass system. The observation of such a large asymmetry has been reported recently [3,4] and found to be in agreement with theoretical predictions. In the case of the short-lived neutral kaon, the decay amplitude is largely dominated by the CP-even inner bremsstrahlung component. Thus, no significant asymmetry in the Φ distribution is expected in the $K_S \to \pi^+\pi^-e^+e^-$ decay. The branching ratio value for the $K_S \to \pi^+\pi^-e^+e^-$ process can be related to the one of the $K_L \to \pi^+\pi^-e^+e^-$ inner bremsstrahlung contribution [1,2] and is predicted to be about two orders of magnitude larger than the recently measured $K_L \to \pi^+\pi^-e^+e^-$ branching ratio [5].

We present in this letter a first determination of the branching ratio of the $K_S \to \pi^+\pi^-e^+e^-$ decay based upon the 1998 data collected by the NA48 experiment at CERN during a 120 day long run dedicated to the measurement of $\mathrm{Re}(\varepsilon'/\varepsilon)$.

2. The NA48 kaon beams and detector layout

The principle of the NA48 experiment relies on the use of simultaneous and almost collinear K_L and K_S beams. Both neutral kaon beams are produced by 450 GeV/c protons extracted from the CERN SPS. The primary proton beam, with a nominal flux of 1.5×10^{12} particles per SPS pulse (ppp), impinges on a Be target at a downward angle of 2.4 mrad to produce the K_L beam. Part of the non-interacting primary protons are deflected towards a bent Si crystal [6]. A small fraction of these protons are channeled by the crystal and deflected back onto the K_L beam line. The resulting low intensity proton beam ($\approx 3 \times 10^7$ ppp) is then transported towards a second 40 cm long, 2 mm diameter, Be target for the production of the K_S beam.

The K_S target is positioned 7.2 cm above the K_L beam axis and 120 m downstream of the K_L target. The K_S collimator selects secondary neutral particles at a 4.2 mrad production angle with a divergence of ± 375 μrad. The K_S beam enters the fiducial decay volume 6.84 cm above the K_L beam. The axes of the two beams cross at the position of the electromagnetic calorimeter with a convergence angle of 0.6 mrad. The total flux per pulse of K_L in the K_L beam entering the fiducial region is about 2×10^7 and of K_S in the K_S beam about 2×10^2.

The protons directed to the K_S target are detected by a tagging detector made of two arrays of thin scintillation counters after the Si crystal [7]. This device is used to tag K_S decays by measuring very accurately the time difference between a proton in the tagging detector and an event in the main detector. Both times are reconstructed relative to a common clock running at 40 MHz. The signals of the tagging detector are digitized by 960 MHz FADCs. The proton time resolution obtained at a proton rate of 28 MHz is about 120 ps and the double-pulse separation is 4 ns.

The decay volume lies inside a large, 90 m long, vacuum tank terminated by a 0.3% radiation lengths thick Kevlar window. The beginning of the decay region is precisely defined on the K_S beam by an anticounter (AKS) which detects all K_S decays occurring further upstream. Starting at the centre of the Kevlar window, a 16 cm diameter vacuum beam pipe traverses all the detector elements to let the neutral beam pass through vacuum.

The layout of the main detector is shown in Fig. 1. Only those elements relevant to the analysis presented here are described below. The detection of the $K_S \to \pi^+\pi^-e^+e^-$ decays is performed using a high resolution magnetic spectrometer which consists of a dipole magnet with a horizontal transverse momentum kick of 265 MeV/c and a set of four drift chambers [8]. Two of them are located upstream of the magnet for the measurement of the decay vertex position whereas the other two, located downstream of the magnet, are used for the bending angle determination of the tracks. The magnetic spectrometer is contained inside a tank filled with helium in order to reduce multiple scattering. Each chamber contains 8 planes of sense wires oriented in four different directions 0° (X, X'), 90° (Y, Y'), −45° (U, U') and +45° (V, V'), orthogonal to the beam axis. In DCH3, only horizontal and vertical wire planes are instrumented. The space resolution in each transverse coordinate is 90 μm and the average efficiency per plane is better than 99%. The momentum determination of a track is achieved with a resolution given by

$$\frac{\sigma_p}{p}(\%) \approx 0.5 \oplus 0.009\, p\ (\mathrm{GeV}/c). \tag{1}$$

The precise time reference of tracks is provided by two planes of a scintillator hodoscope located downstream of the last drift chamber. The time resolution is about 200 ps per track.

The e/π identification is obtained by comparing the momentum p of a track measured by the magnetic spectrometer with the energy E deposited in a quasihomogeneous liquid krypton (LKr) calorimeter [9]. This detector has a 127 cm long projective tower structure which is made of copper–beryllium

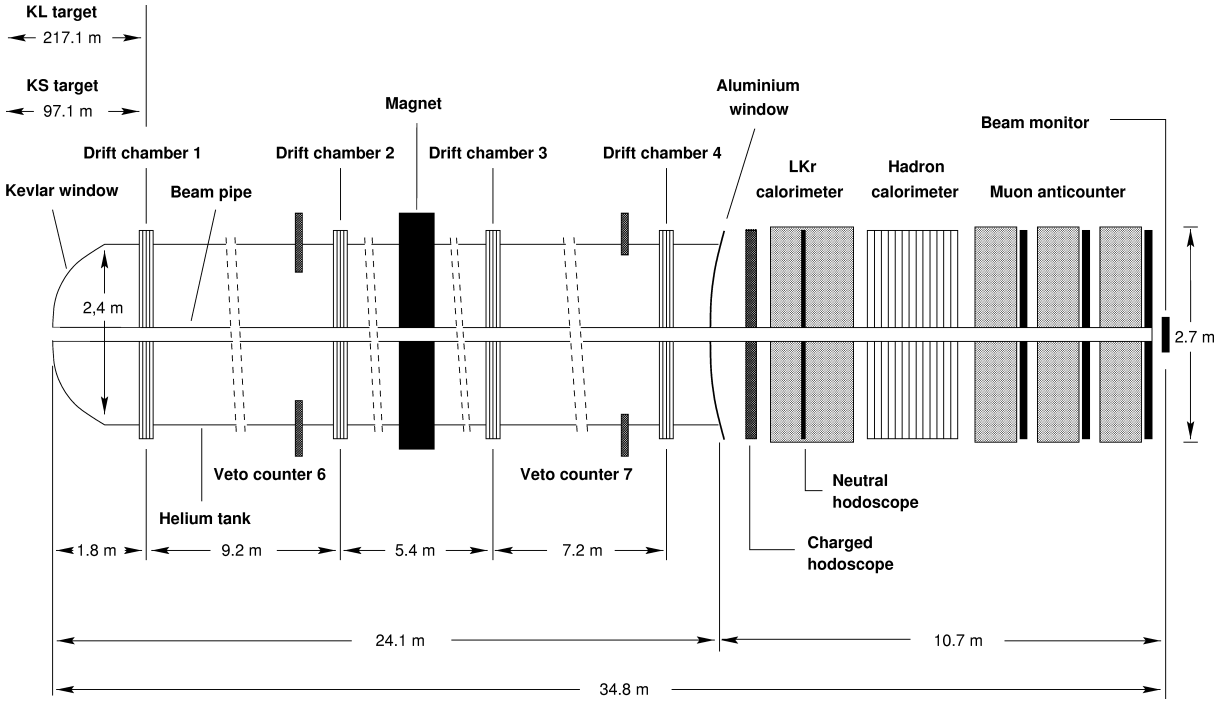

Fig. 1. Layout of the NA48 detector.

ribbons extending between the front and the back of the calorimeter with a ±48 mrad accordion geometry. The 13212 readout cells each have a cross section of 2×2 cm^2 at the back of the active region. The initial value of the current induced on the electrodes by the drift of the ionisation is measured using 80 ns FWHM pulse shapes digitized with 40 MHz FADCs. The energy resolution of the calorimeter is

$$\frac{\sigma_E}{E}(\%) \approx \frac{3.2}{\sqrt{E}} \oplus \frac{10.0}{E} \oplus 0.5 \quad (E \text{ in GeV}). \tag{2}$$

The time and spatial resolutions achieved for 20 GeV photons are better than 300 ps and 1.3 mm, respectively.

Behind the LKr calorimeter, a 6.7 nuclear interaction lengths thick calorimeter made of iron and scintillator is used to provide the energy of hadrons in the trigger. Finally, a set of three planes of 25 cm wide scintillation counters shielded by 80 cm thick iron walls is used to veto muons.

In 1998, a specific algorithm was implemented in the Level 2 charged trigger (L2C) to select events compatible with decays into four charged particles, concurrently with the ε'/ε trigger [10]. The L2C trigger performs a fast tracking of charged particles in the spectrometer. It receives signals from the earlier Level 1 (L1) trigger stage which demands a minimum number of hits in DCH1 and in the scintillator hodoscope compatible with at least 2 tracks, together with a total energy seen in the electromagnetic and hadronic calorimeters greater than 35 GeV.

The 4-track trigger requires at least two compatible 2-track vertices within 9 m along the longitudinal kaon direction and at least three reconstructed space-points in each drift chamber 1, 2 and 4. No requirement on the invariant mass of the selected events is made. In order to determine the efficiency of the 4-track trigger, down-scaled events that passed the L1 condition were recorded with a control trigger. The trigger inefficiency due to the algorithm itself is 3%. However, about 25% of good 4-track events were lost owing to the maximum latency of 102.4 μs allocated to process the events. In addition, an extra 10% contribution to the trigger inefficiency comes from accidental electromagnetic showers generated upstream of the drift chambers that produce high multiplicity events in the spectrometer. Such events generate an overflow condition which resets the front-end readout buffers when more than 7 hits per plane are present within a 100 ns time interval [11]. The overall 4-track trigger efficiency during the 1998 run was about 65%. The output rate of the 4-track trigger was 1 k events per SPS cycle, representing about 5% of the total data flow of the experiment.

3. Event selection and background rejection

The offline selection of $K_S \to \pi^+\pi^-e^+e^-$ candidates requires four in time tracks from particles hitting the LKr calorimeter to allow for particle identification. All four tracks are required to impinge on the detector sufficiently far from the beam pipe and the outer radius ($15 < R_{LKr} < 120$ cm) to ensure efficient electron identification with negligible energy losses. In addition, tracks with an impact point closer than 2 cm from a dead calorimeter cell are rejected. Electrons are identified by requiring $0.85 \leqslant E/p < 1.15$ while tracks are designated as pions if they have $E/p < 0.85$ and no associated hit in coincidence in the Muon Veto detector. We demand also that both the electron and pion pairs have two particles of opposite charge and that the reconstructed momentum of each track be above 2 GeV/c.

A vertex made of four tracks passing the above cuts is formed if each of the six combinations of pairs of tracks has a distance of closest approach smaller than 10 cm and a reconstructed vertex located upstream of the Kevlar window. To reject fake vertices made of two overlapping decays, a χ^2 value smaller than 50 was required as a vertex quality cut. Background events coming from $K_S \to \pi^+\pi^-\gamma$ decays followed by a gamma conversion in the Kevlar window are further suppressed by imposing a 2 cm separation between the two electron tracks in the first drift chamber.

Events originating from decays in the K_L beam are separated by requiring the 4-track vertex transverse position to be more than 4 cm above the K_L beam axis. The resolutions on the transverse and longitudinal positions of the 4-track vertex are typically 1.8 mm and 55 cm, respectively.

$K_S \to \pi^+\pi^-e^+e^-$ candidates are accepted if the kaon energy is larger than 40 GeV and if its momentum vector, extrapolated upstream to the exit face of the final collimator, is contained within a 2.5 cm radius around the K_S collimator hole. In order to help

to remove unwanted events due to decays in the high intensity K_L beam, a ± 1 ns cut on the time difference between the event and the signal from the K_S tagging detector is applied. This analysis cut removes less than 1% of good events but provides an extra factor of 20 in the background suppression from the K_L beam.

To remove events from K_S scattering in the collimators or the AKS, we require the centre of energy of the four tracks, extrapolated at the LKr calorimeter position, to lie within 8 cm of the beam axis. This cut is chosen relatively wide compared to the 4.6 cm K_S beam spot radius. Moreover, events having hits in coincidence in the AKS counter are rejected.

Events from the dominant $K_S \to \pi^+\pi^-$ decay mode in time with gamma conversions in the collimators or the detector material in front of the first chamber are eliminated if the $\pi^+\pi^-$ invariant mass is measured to be between $490.7 < M_{\pi\pi} < 504.7$ MeV/c^2. Accidental background is further reduced by rejecting events with an extra track measured in the spectrometer within 1 ns around the event time.

Since equal amounts of K_S and K_L are produced at the target, a potential source of background to $K_S \to \pi^+\pi^- e^+e^-$ comes from $K_L \to \pi^+\pi^-\pi^0_D$ decays where the extra photon from the π^0 Dalitz decay ($\pi^0 \to e^+e^-\gamma$), denoted π^0_D here, is not detected. Most events with a missing particle are suppressed by demanding that the square of the total momentum $P_\perp^2$ of the observed decay products relative to the line of flight of the parent kaon be less than 0.02 GeV$^2/c^2$.

Finally, rejection of $\Xi^0 \to \Lambda\pi^0_D$ decays is obtained by removing events compatible with a $\Lambda \to p\pi$ decay. Four-track candidates with the two hadrons having a $p\pi$ invariant mass within 4 MeV/c^2 around the Λ mass value are eliminated.

The invariant mass distribution $M_{\pi\pi ee}$ of the remaining candidates, after all the above selection criteria have been applied, is shown in Fig. 2. The number of accepted $K_S \to \pi^+\pi^- e^+e^-$ events which are required to lie in the $477.7 < M_{\pi\pi ee} < 512.7$ MeV/c^2 range is found to be 56. The background contamination due to $K_L \to \pi^+\pi^-\pi^0_D$ decays with a missing photon is negligible and has been estimated to be 0.3 ± 1.0. The e^+e^- invariant mass M_{ee} distribution for the signal events is shown in Fig. 3. It exhibits a steep variation at low mass values as expected from the mechanism of inner bremsstrahlung.

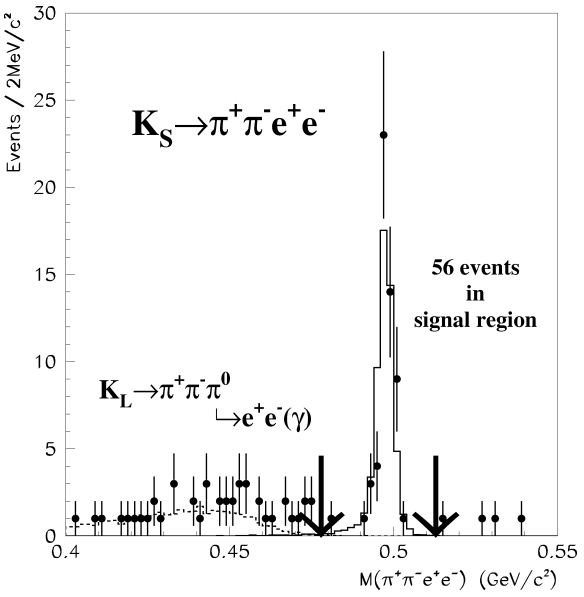

Fig. 2. Measured invariant mass distribution $M_{\pi\pi ee}$ for $K_S \to \pi^+\pi^- e^+e^-$ event candidates (solid dots). The solid line is the predicted Monte Carlo distribution of $K_S \to \pi^+\pi^- e^+e^-$ events, normalized to the number of good events observed in the data. The arrows indicate the accepted mass region for good events. The dashed line is the Monte Carlo prediction for $K_L \to \pi^+\pi^-\pi^0_D$ events, after normalization to the flux of K_L decays from the data sample (see text).

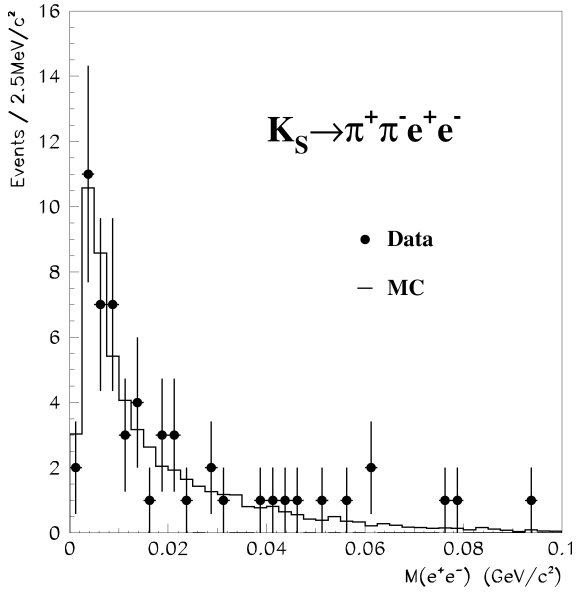

Fig. 3. Invariant mass distribution M_{ee} for $K_S \to \pi^+\pi^- e^+e^-$ events (solid dots). The solid line is the Monte Carlo prediction.

To determine the $K_S \to \pi^+\pi^-e^+e^-$ branching ratio, $K_L \to \pi^+\pi^-\pi^0_D$ decays from K_L produced in the K_S target are used as normalization. Although the expected number of such events in the decay region is only a factor of two larger than the signal one, this choice for the normalization has the advantage that inefficiencies in the trigger or in the event reconstruction cancel to first order. However, due to the very different lifetimes of the short- and long-lived neutral kaons, the relative K_S to K_L flux in the fiducial decay region of the experiment has to be determined precisely.

The selection of $K_L \to \pi^+\pi^-\pi^0_D$ events is very similar to the one done for the $K_S \to \pi^+\pi^-e^+e^-$ events. We demand, in addition to the four identified charged particles, the presence of an isolated cluster in the LKr calorimeter, in time with the event and with an energy greater than 2 GeV, well above the detector noise of 100 MeV per cluster. The transverse distance of the cluster to a dead cell is required to be greater than 2 cm and the distance to any of the four impact points of the charged particles on the LKr to be greater than 15 cm. $K_L \to \pi^+\pi^-\pi^0_D$ candidates are accepted if the reconstructed $e^+e^-\gamma$ invariant mass is between 110 and 150 MeV/c^2 and if the $\pi^+\pi^-e^+e^-\gamma$ invariant mass lies in the 477.7 to 512.7 MeV/c^2 range. The $P_\perp^2$ value of the reconstructed $\pi^+\pi^-e^+e^-\gamma$ final state is required also to be less than 0.02 GeV$^2/c^2$. A total of 105 $K_L \to \pi^+\pi^-\pi^0_D$ events with a kaon energy greater than 40 GeV have been identified in the fiducial region comprised between the AKS position ($z = 0$) and $z = 84$ m. The contamination from $K_L \to \pi^+\pi^-\pi^0_D$ decays in the K_L beam has been estimated to be 1.5 ± 0.2 from the study of the accidental activity in the tagging detector. Fig. 4 shows the comparison of the proper decay time distributions for the signal and the normalization events.

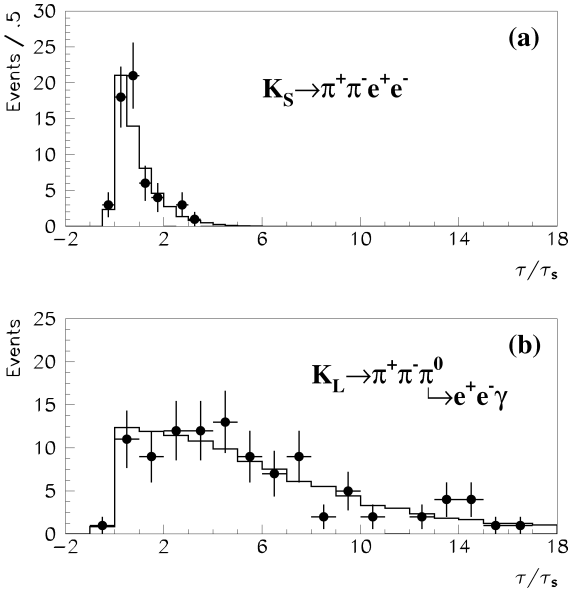

Fig. 4. Proper decay time distribution τ/τ_S in units of the K_S lifetime τ_S for (a) the $K_S \to \pi^+\pi^-e^+e^-$ mode and (b) the $K_L \to \pi^+\pi^-\pi^0_D$ mode. The histograms are the Monte Carlo distributions normalized to the corresponding observed numbers of events.

4. Branching ratio determination

The branching ratio for $K_S \to \pi^+\pi^-e^+e^-$ normalized to the one from $K_L \to \pi^+\pi^-\pi^0_D$ decays can be written as

$$\frac{\mathrm{BR}(K_S \to \pi^+\pi^-e^+e^-)}{\mathrm{BR}\left(K_L \to \pi^+\pi^-\pi^0_D\right)} = \frac{N_{\pi\pi ee}}{N_{\pi\pi\pi^0_D}} \frac{A_{\pi\pi\pi^0_D}}{A_{\pi\pi ee}} \frac{\epsilon_{\pi\pi\pi^0_D}}{\epsilon_{\pi\pi ee}} \frac{\phi_L}{\phi_S}, \quad (3)$$

where $N_{\pi\pi ee}$ and $N_{\pi\pi\pi^0_D}$ are respectively the number of signal and normalization events after background subtraction, $A_{\pi\pi ee}$ and $A_{\pi\pi\pi^0_D}$ are the corresponding acceptance corrections, $\epsilon_{\pi\pi ee}$ and $\epsilon_{\pi\pi\pi^0_D}$ the trigger efficiencies, and ϕ_S and ϕ_L are, respectively, the fractions of K_S and K_L with energy above 40 GeV decaying in the fiducial region. The branching ratio $\mathrm{BR}(K_L \to \pi^+\pi^-\pi^0_D) = [1.505 \pm 0.047] \times 10^{-3}$ has been obtained from the existing data on $\mathrm{BR}(K_L \to \pi^+\pi^-\pi^0)$ and $\mathrm{BR}(\pi^0 \to e^+e^-\gamma)$ [12].

In order to determine the kaon decay probabilities ϕ_S and ϕ_L, an analysis of the kaon production spectrum has been performed using the abundant $K_S \to \pi^+\pi^-$ sample measured with the down-scaled L1 triggers. Taking into account the K_S and K_L lifetime values, ϕ_S and ϕ_L are found to be 26.2% and 3.46%, respectively.

The detector acceptances have been estimated using a detailed Monte Carlo simulation based on GEANT [13]. For the generation of $K_S \to \pi^+\pi^-e^+e^-$ events, the model of Ref. [2] for the inner bremsstrahlung

contribution has been used after taking into account the correct M_{ee} dependence of the differential decay rate and keeping the electron mass terms in the matrix element [14]. Radiative corrections, for both the signal and the normalization channels, have been included in the acceptance calculation using the PHOTOS code [15]. The acceptances for $K_S \to \pi^+\pi^-e^+e^-$ and $K_L \to \pi^+\pi^-\pi^0_D$ are determined to be 3.70% and 1.56%, respectively.

The trigger efficiency $\epsilon_{\pi\pi\pi^0_D}$ for the normalization channel has been studied using the large sample of fully reconstructed $K_L \to \pi^+\pi^-\pi^0_D$ events seen in the K_L beam line that was collected with the down-scaled control trigger. The measured efficiency of the trigger algorithm is found to be 0.97 ± 0.02 in good agreement with the result of 0.98 obtained from the trigger simulation. For the signal channel, the limited statistics do not permit to measure directly the efficiency of the trigger. We rely instead on the simulation of the trigger algorithm. Possible differential losses in the trigger due to accidental high multiplicity events creating overflows in the drift chambers have also been investigated using the more abundant $K_L \to \pi^+\pi^-e^+e^-$ and $K_L \to \pi^+\pi^-\pi^0_D$ decays in the K_L beam. Such effects have been found to be smaller than 5%. The relative trigger efficiency ratio $\epsilon_{\pi\pi\pi^0_D}/\epsilon_{\pi\pi ee}$ between the normalization and signal channels has been determined to be 1.01 ± 0.05.

Using the above corrections, we obtain a branching ratio of

$$\mathrm{BR}(K_S \to \pi^+\pi^-e^+e^-) = [4.5 \pm 0.7(\mathrm{stat}) \pm 0.4(\mathrm{syst})] \times 10^{-5}. \quad (4)$$

The stability of the branching ratio determination with respect to moderate changes of the selection criteria is found to be about 5%. Other contributions to the systematic error are due to the uncertainties on the kaon spectra, beam fluxes and acceptances (6%), on the trigger inefficiencies (5%), and on the branching ratio $\mathrm{BR}(K_L \to \pi^+\pi^-\pi^0_D)$ (3%). The total systematic error on the measured branching ratio has been obtained by adding in quadrature the above contributions.

Our result translates into a value of $\mathrm{BR}(K_L \to \pi^+\pi^-e^+e^-) = [1.4 \pm 0.2] \times 10^{-7}$ for the inner bremsstrahlung component of the $K_L \to \pi^+\pi^-e^+e^-$ decay, in good agreement with theoretical predictions [1,2,14].

Acknowledgements

We would like to thank the technical staff of the participating laboratories, universities and affiliated computing centres for their efforts in the construction of the NA48 detector, in the operation of the experiment and in the processing of the data. We are also indebted to L.M. Sehgal for fruitful discussions on the theoretical aspects of the $K_{L,S} \to \pi^+\pi^-e^+e^-$ process.

References

[1] L.M. Sehgal, M. Wanninger, Phys. Rev. D 46 (1992) 1035, Erratum: Phys. Rev. D 46 (1992) 5209.
[2] P. Heiliger, L.M. Sehgal, Phys. Rev. D 48 (1993) 4146, Erratum: Phys. Rev. D 60 (1999) 079902.
[3] A. Alavi-Harati et al., Phys. Rev. Lett. 84 (2000) 408.
[4] S. Wronka et al., Talk given at the KAON99 Conference, Chicago, IL, USA, 1999.
[5] J. Adams et al., Phys. Rev. Lett. 80 (1998) 4123.
[6] N. Doble et al., Nucl. Instrum. Methods B 119 (1996) 181.
[7] P. Grafström et al., Nucl. Instrum. Methods A 344 (1994) 487; H. Bergauer et al., Nucl. Instrum. Methods A 419 (1998) 623.
[8] D. Bédérède et al., Nucl. Instrum. Methods A 367 (1995) 88.
[9] M. Martini et al., in: Proc. 7th Int. Conf. on Calorimetry in High Energy Physics, Tucson, AR, USA, World Scientific, 1997, p. 375.
[10] S. Anvar et al., Nucl. Instrum. Methods A 419 (1999) 686; S. Anvar et al., Proc. 1998 IEEE Nuclear Science Symposium, Toronto, ON, Canada. http://www-dapniaI2.cea.frr:80/Doc/Publications/PreprintDapnia-99-06
[11] I. Augustin et al., Nucl. Instrum. Methods A 403 (1998) 472.
[12] Particle Data Group, Eur. Phys. J. C 3 (1998) 459; Particle Data Group, Eur. Phys. J. C 3 (1998) 357.
[13] CERN Program Library Long Writeup W5013, 1993.
[14] The correct expression of the differential decay rate for the $K_L \to \pi^+\pi^-e^+e^-$ process is obtained by replacing in Eq. (13) of Ref. [2] the kinematic factor $(1 - 4m^2/s_l)^2$ by $(1 - 4m^2/s_l)^{1/2}$. The inclusion of the electron mass terms in the matrix element for he $K_S \to \pi^+\pi^-e^+e^-$ process brings an extra correction on the branching ratio of about 4%.
[15] E. Barbario et al., Comput. Phys. Commun. 66 (1991) 115.